

# EXPLORING THE USE OF HPFRC AND GFRP GRIDS FOR THE PRODUCTION OF MANHOLE COVERS

OÑA Mónica <sup>1</sup>, SOLTANZADEH Fatemeh <sup>2</sup>, DE SOUSA Christoph <sup>2</sup>,  
 BARROS Joaquim A. O. <sup>3</sup>

## Abstract

*Corrosion of the steel reinforced concrete elements is one of the common pathologies that limits the long-term performance of urban infrastructures. This problem causes the loss of structural serviceability by decreasing the concrete-steel bond strength and reducing the cross section of the reinforcements. The present study introduces a new system for developing free-corrosion resistance prefabricated manhole covers for applications in the aggressive environments, i.e. wastewater collector systems, sewer systems, stormwater systems, etc. Fibre reinforced cement composites were applied in this system in order to suppress the corrodible steel mesh and maintain the structural ductility as well. Application of fibre reinforced polymer (FRP) system is adopted as the additional solution for increasing the load carrying capacity of these elements without concerns about corrosion. The effectiveness of the applied strategy in developing the manhole covers in terms of load carrying capacity and failure mode is evaluated in this research. Furthermore, this paper discusses a FEM-based simulation, aiming to address the possibility of calibrating the constitutive model parameters related to fracture modes I and II.*

**Keywords:** Fibre reinforced cement composites, Discrete fibres, FRP reinforcements, Free-corrosion manhole covers, Finite element simulation

## 1. Introduction

Urban infrastructures such as manhole covers for wastewater collector systems, sewer systems and stormwater systems have been made of steel, due to its high resistance, durability and little maintenance requirements. However, due to its high economic value in the construction field, steel manhole covers have been stolen in several sidewalks and roads of many countries, in order to sell them as scrap. In 2012, the New York Times reported that based on the current commodity prices for iron and steel, a stolen manhole cover might fetch more than \$30, but it costs the municipality about \$200 to replace each

---

<sup>1</sup> OÑA Mónica, [moni.ona.vera@gmail.com](mailto:moni.ona.vera@gmail.com)

<sup>2</sup> SOLTANZADEH Fatemeh, [soltanzadehfaranak@gmail.com](mailto:soltanzadehfaranak@gmail.com)

<sup>3</sup> DE SOUSA Christoph,, [christoph@civil.uminho.pt](mailto:christoph@civil.uminho.pt)

<sup>4</sup> BARROS Joaquim A. O., [barros@civil.uminho.pt](mailto:barros@civil.uminho.pt)

<sup>1,2,3,4</sup>ISISE, Dep. Civil Eng., Minho Univ., Campus Azurém 4800-058 Guimarães, Portugal,

one, not counting the labour involved [1]. In China, the BBC reported 1826 manhole covers were stolen in 45 days, causing a loss of about 66k€[2]. However, even worse than the economic harm, manholes without covers endanger the lives of pedestrians, especially at night, and children or those people with poor sight. In fact, a BBC publication reported that eight people had fallen down uncovered holes and died in China in less than 6 months [2]. Although some governments of Asian Countries like India and China have taken the initiative of replacing the steel manhole covers with concrete covers, in order to give an end to this situation, the thefts persisted, since the concrete covers were also stolen for the rebar inside the concrete [3].

The present paper presents an extended experimental program aimed to study different possibilities to give a short-term and cost-effective solution to these misdeeds. The use of a Fibre Reinforced Polymer (FRP) grid as a reinforcement system inside two different concrete compositions is being explored. Due to its non-recyclable value, the polymeric system is a suitable proposal to substitute the steel covers and the concrete covers reinforced with steel bars, thus, eliminating the attraction of stealing them. The concrete mixes proposed for their production are fibre reinforced cement composites of high rheological and mechanical properties, that will enhance the shear and compressive strength of the suggested prototypes. Moreover, these concrete mixes have been tailored to ease the manufacturing process for the massive production of precast manhole covers in the industry [4, 5].

Finally, besides the experimental program, the applicability of a multidirectional fixed smeared crack constitutive model on the three-dimensional numerical simulation of a representative specimen has been studied. The specimen, the loading and the support conditions were simulated following the experimental set up specifically developed for this experimental program.

## 2. Experimental Program

### 2.1 Specimens and materials

Two types of cement-based materials were adopted for the production and experimental study of four manhole covers: i) Deflection Hardening Cement Composite (DHCC), used for the first two specimens, and ii) High Performance Fibre Reinforced Concrete (HPFRC), adopted for the third and fourth specimens. The mixture composition developed for the DHCC [5] used for the first two specimens is presented in Tab. 1 and includes a hybrid fibre reinforcement system, totalizing a total fibre volume content of 4% (3% of PAN12 and 1% of PAN6 synthetic fibres, whose relevant properties are indicated in Tab. 2).

Tab. 1: Mixture composition for the DHCC

Cement	500 kg/m <sup>3</sup>
Fly ash	500 kg/m <sup>3</sup>
Lime stone filler	90 kg/m <sup>3</sup>
Sand	200 kg/m <sup>3</sup>
Admixture (superplasticizer and viscosity modification agent)	33 L/m <sup>3</sup>
Water	388 L/m <sup>3</sup>

Tab. 2: Properties of the PAN fibres included in the DHCC composition

Fibre	Length [mm]	Diameter [ $\mu\text{m}$ ]	Elasticity modulus [MPa]	Tensile strength [MPa]	Density [ $\text{g}/\text{cm}^3$ ]	Elongation [%]
PAN6	6	58	9910	564	1.17	13-17
PAN12	12	26	6856	264.4	1.17	14-18

The second set of manhole covers was casted implementing an enhanced self-compacting concrete (SCC) suitable for the production of precast manhole covers. This material includes a hybrid fibre reinforcement system formed by polypropylene and steel fibres, and has self-compacting character.). This concrete technology is currently being subjected to a patent process and, therefore, due to confidentiality reasons, its mixture composition cannot be revealed in this research paper. Nevertheless, the average material properties of the HPFRC at the age 28 days are given in Tab. 3. The concepts of residual flexural strength and limit of proportionality are defined in the CEB-FIP Model Code 2010.

Tab. 3: HPFRC material properties

Compressive strength ( $f_c$ )	57.3 $\text{N}/\text{mm}^2$
Young's modulus ( $E$ )	35 583 $\text{N}/\text{mm}^2$
Residual flexural strength:	
CMOD1 (0,5)	13.23 $\text{N}/\text{mm}^2$
CMOD2 (1,5)	13.09 $\text{N}/\text{mm}^2$
CMOD3 (2,5)	11.73 $\text{N}/\text{mm}^2$
CMOD4(3,5)	10.22 $\text{N}/\text{mm}^2$
Limit of proportionality (at $\delta_L = 0.05 \text{ mm}$ )	8.45 $\text{N}/\text{mm}^2$

In addition to the aforementioned concrete solutions, a FRP grid system was adopted as the main reinforcement of the manhole cover prototypes. The grid was embedded in the concrete mixture, both for the DHCC and HPFRC specimens (Fig. 2) and placed over a concrete cover of different thicknesses ( $t=15\text{mm}$ ,  $25\text{mm}$  and  $30\text{mm}$ ), involving an upper concrete layer of  $t_{\text{ucf}}= 50\text{mm}$ ,  $30\text{mm}$ ,  $20\text{mm}$  and  $35\text{mm}$ , depending on the thickness of the correspondent specimen. These differences in the upper concrete layer thicknesses is of significance in the behaviour of the specimens during the tests, as it will be explained further on, in sec. 2.3.

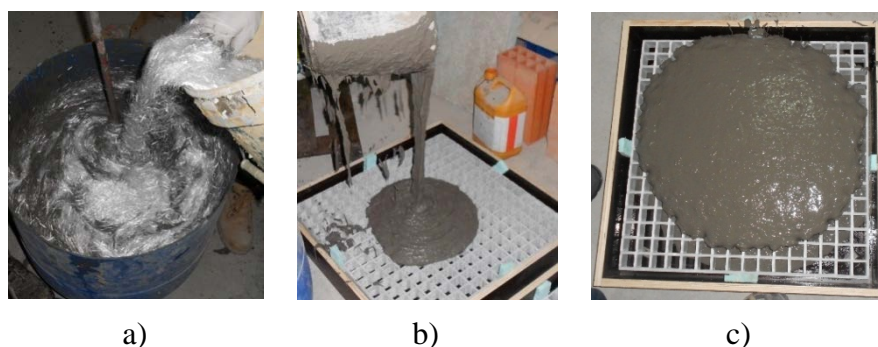


Fig. 1: Casting process for the DHCC specimens: a) mixing the fibres in the cement-based matrix; b) pouring the concrete in the mould; c) concrete flowing through the holes of the FRP grid

The four specimens of this experimental program have a square geometric configuration, with an area of 645x645 mm<sup>2</sup>, designed for clear opening of 600 mm. The differences between specimens are the concrete matrix (different concrete solutions were adopted), the overall thickness and the thickness of the concrete cover (below and above the FRP grid). Tab. 4 presents the designation adopted for the specimens, which is systematized as follows: the first set of letters correspond to the type of concrete adopted for the production of the manhole covers (DHCC or HPFRC); the second set denotes the total thickness of the specimen (T) and the last set refers to the thickness of the concrete cover existent below the reinforcement (C). Additional details regarding the geometry, thickness and concrete covering are shown in Fig. 3. Besides the referred manhole covers, cylindrical and prismatic specimens for standard characterization tests were also casted.

Tab. 4: Details of the specimens studied in the experimental program

Specimen designation	Dimensions [mm <sup>2</sup> ]	Total thickness [mm]	Concrete cover [mm]
DHCC-T80-C15	645x645	80	15
DHCC-T100-C15	645x645	100	15
HPFRC-T80-C25	645x645	80	25
HPFRC-T100-C30	645x645	100	30

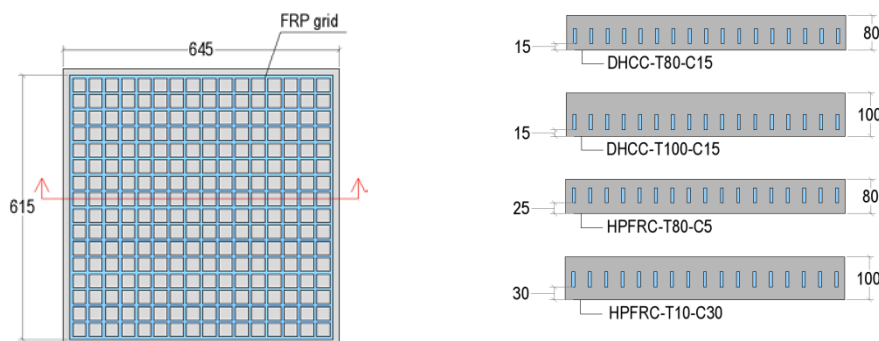


Fig. 2: Manhole cover prototypes dimensions and cross-section in mm

## 2.2 Test setup and procedure

A special support was designed to be used as part of the test setup, with a clear opening of 600 mm diameter, as depicted in Fig. 3a. This apparatus also included: i) openings in each lateral side of the concrete base, in order to allow access to its inner part during the experimental tests (to install or remove displacement transducers) and ii) an additional 5 mm thick steel support (see Fig. b) to be placed on its upper surface, as depicted in Fig. c, in order to avoid direct contact between the specimens and the concrete block, preventing any possible deterioration in the referred surface due to abrasion/friction effect in the tests.

In the particular case of Portugal, the manholes (chamber for access shaft to underground wastewater systems) existent in pedestrian and vehicular traffic areas have commonly a clear opening (CO) of 600 mm. Therefore, in order to reproduce with high accuracy the real condition on which the manhole cover would be working, a special support was designed to be used as part of the test setup, with a CO=600 mm diameter, (Fig. 3a). This base also included: i) openings in each lateral side of the concrete base, in order to allow access to its inner part during the experimental tests (i.e., in order to install or remove displacement transducers) and ii) an additional 5 mm thick steel support (see Fig. 3b) to be placed on its upper surface, as depicted in Fig. 3c, in order to avoid direct contact between the specimens and the concrete block, preventing any possible deterioration in the referred surface due to abrasion/friction effect.

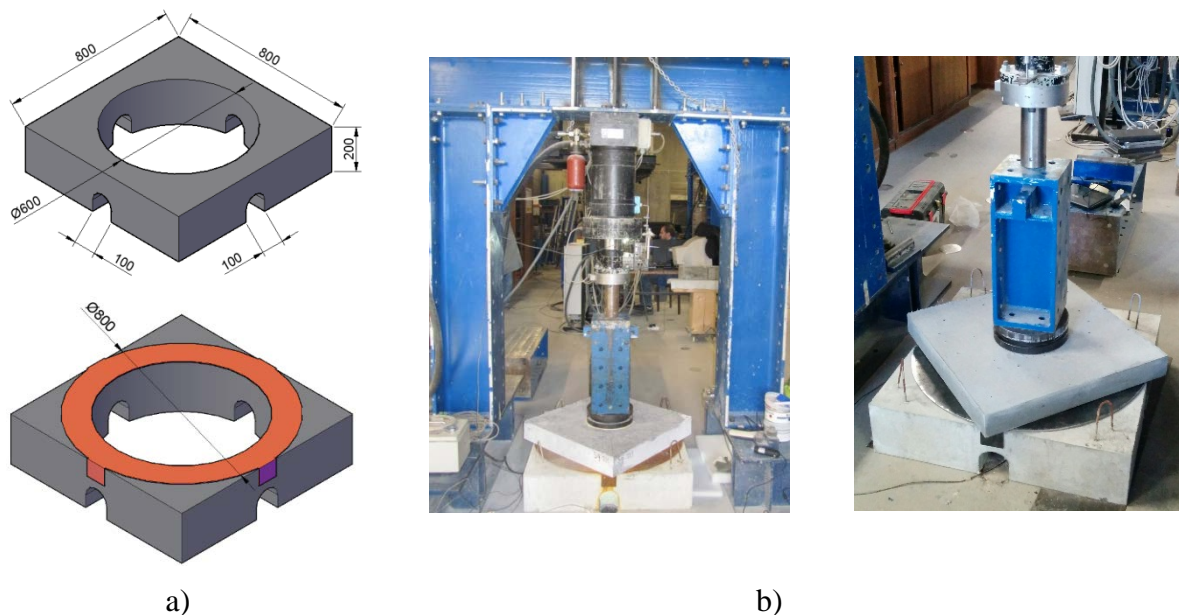


Fig. 3: a) concrete base and steel support; b) testing frame, actuator and specimen.

All the specimens were tested by using a servo-hydraulic actuator of 500kN capacity (Fig. 4a), displacement controlled at a rate of  $1 \mu\text{m/s}$ . The load was applied on the geometric centre of the manhole covers, uniformly distributed in a circular area defined by a diameter of 250 mm (5b and 5c), as specified in the EN-124 [6]. The vertical deflection was measured using a Linear Variable Differential Transducer (LVDT) placed at the bottom of the specimens, aligned with its geometric centre.



During the experimental procedure the goal was to assess the maximum load carrying capacity of the specimens, and compare these values to the test loads (see Tab. 5) defined in the EN-124, which establishes the classes of utilization, design and testing requirements for the production of gully and manhole covers covers intended to be installed in areas subjected to pedestrian and/or high vehicular traffic.

Tab. 5: Test loads and classes of utilization defined in the EN-124 [2]

Class of utilization	Test load [kN]
A 15	15
B 125	125
C 250	250
D 400	400
E 600	600
F 900	900

### 2.3 Experimental results

To evaluate and compare the performance of the specimens, Load–Deflection curves are analysed. A comparison between the results obtained from the DHCC specimens suggests that a higher load and a stiffer behaviour, in the elastic part of the curve, are achieved with the increase of the thickness of the concrete layer above the FRP reinforcement. The specimen with 50mm of thickness in the upper concrete layer ( $t_{ucl}$ ), DHCC-T100-C15, has reached a maximum load carrying capacity of 156 kN at  $\delta=8.1$ mm, whereas that the specimen with  $t_{ucl}=30$ mm (DHCC-T80-C15) has achieved 128 kN at  $\delta=13$ mm.

The second part of the curve (after the peak load) evidences a very ductile behavior with a maximum load decay of 23% and 17% for specimens with  $t_{ucl}=50$ mm and  $t_{ucl}=30$ mm, respectively. These decays remain constant up to the end of the tests, evidencing a suitable post peak performance as part of the pseudo-plastic region of the curve (see Fig.4).

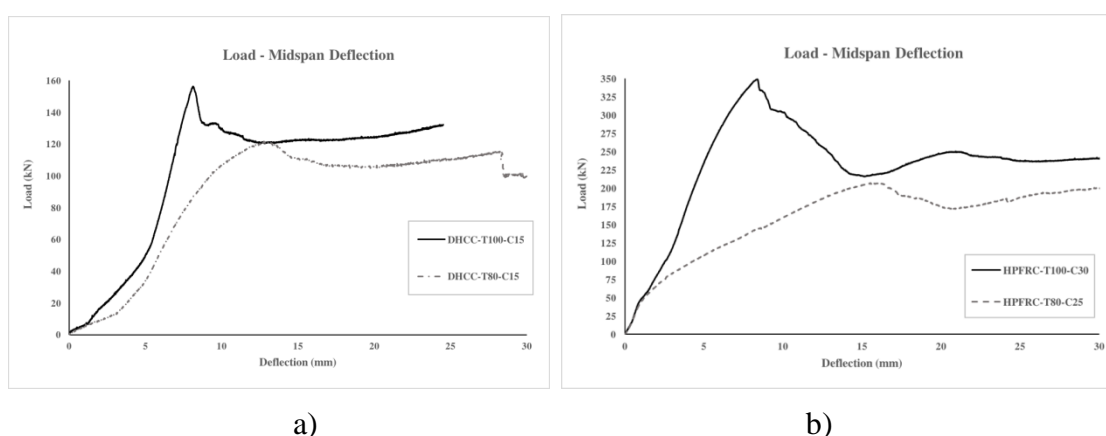


Fig. 4: Experimental curves obtained for a) DHCC and b) HPFRC specimens

On the other hand, a comparison between the HPFRC and DHCC specimens of the same thickness evidences the significant effect of concrete matrix on the behaviour and load carrying capacity of the specimens. As shown in Fig. 5 manhole covers of HPFRC achieved a maximum load carrying capacity of 349 kN and 208 kN for specimens of 100 mm and 80 mm thickness, respectively. The value of the vertical deflection at the peak load was the same in the case of the specimens of T100 (DHCC-T100-C15 and HPFRC-T80-C30) due to the better material performance of the HPFRC (see Fig. 6). In the manhole covers of T80, although the maximum load achieved was higher for the HPFRC specimen (approximately 1.62 times higher), the deflection was superior as well (3.2 mm of difference). The HPFRC specimen of 100 mm thickness shows a peak load 1.68 times higher than the one achieved by the specimen of 80 mm thickness. Furthermore, the differences in the midspan deflection are quite remarkable (Fig 4), which means that the thickness of the upper layer of concrete ( $t_{ulc}$ ) has a significant role on the performance of the manhole cover system when submitted to the adopted loading configuration. As a conclusion, it is remarkable that the maximum loads of 349.36 kN and 156.32 kN reached by specimens HPFRC-T100-C30 and DHCC-T100-C15 correspond to manhole covers of class C250 and class B125, according to the CEN. EN 124:1994 [6] (Fig 6).

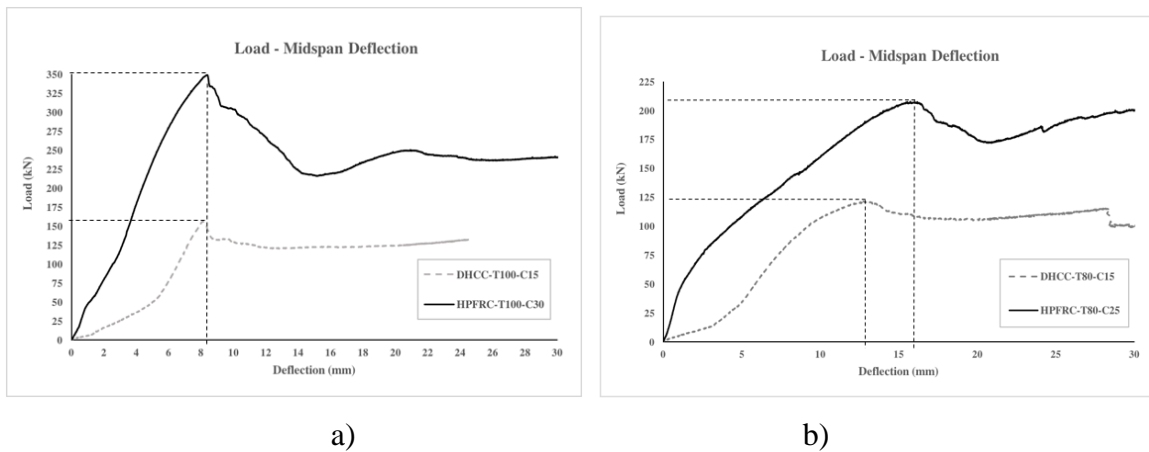


Fig. 5: Comparative experimental L-D curves for specimens a) T100 and b) T80

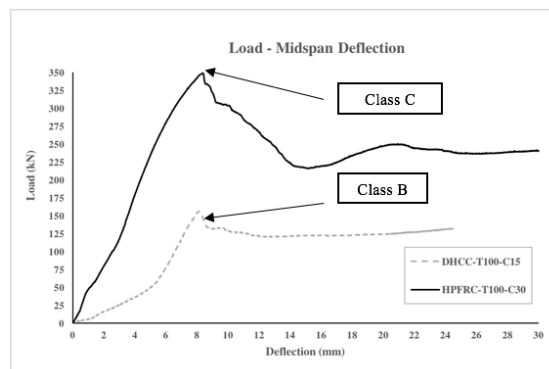


Fig 6: Load – Deflection curve of manhole covers T100

Figure 7a evidences that the DHCC of the first two specimens did not fill all the grid spaces, leaving some gaps that would have negatively affected the maximum load carrying

and the stiffness of the corresponding manhole covers. On contrary, Figure 7b shows that the HPFRC of the second set of specimens filled properly all the grid spaces, which may have contributed for the higher load carrying and stiffness of the corresponding manhole covers.

All the specimens showed multiple cracking behavior at the bottom and top surface, suggesting a ductile behavior. Crack patterns corresponding to punching failure are also observed at the bottom and top surface of the specimens (Fig 7).

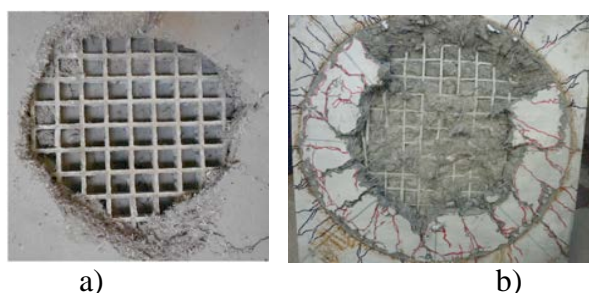


Figure 7. View of the bottom of the specimens, once the concrete cover was removed a) DHCC and b) HPFRC



Figure 8. View of the bottom (L) and top (R) of specimens of a) DHCC and b) HPFRC

### 3. Numerical simulations

A three-dimensional numerical simulation was carried out using the smeared crack model for capturing the relevant features of the specimen HPFRC-T100-C30, which corresponds to manhole covers of class C250 according to the CEN. EN 124:1994 [6]. For a complete description of the formulation of the multi-directional fixed smeared crack model the reader is addressed to [4]. The numerical model, where the specimen, the loading, and the support conditions were simulated in agreement with the experimental test setup, as shown in Fig. 8. Due to symmetry around the centre of the specimen, only a quarter of the specimen was considered. The domain is discretized with 8-noded hexahedral finite elements with an integration scheme of  $2 \times 2 \times 2$  points. The displacement of the nodes along the side boundaries parallel to X-coordinate and Y-coordinate are respectively fixed in the Y and X-direction, while the displacement of those nodes along the bottom boundary is fixed in the Z-direction (see Fig. 9).

The values of the parameters of the constitutive model for HPFRC are summarized in Tab. 6. Since the relatively small size of the edge of the FRP grid mesh caused to place less steel fibres in these locations, the elements modelling these zones were considered constituted by plain concrete. The values of the parameters for the constitutive model for this plain concrete are indicated in Tab 6.



The FRP mesh was modelled using hexahedral finite elements and  $2 \times 2 \times 2$  integration points. These elements were assumed to have a perfect bond with concrete elements. The experimental observation demonstrated that the FRP material exhibits an almost linear behaviour up to its tensile strength, followed by an abrupt rupture. So, to capture this sudden drop, a multi-directional fixed smeared crack model was assigned to these elements (the parameters of the constitutive model were defined to capture this sudden drop as much as possible). The parameters of the constitutive model for the FRP material are presented in Table 6. Figure 10 shows that this modelling strategy was capable to capture with reasonable accuracy the flexural response of this type of specimens. However, there is a tendency for predicting a higher stiffness, peak load and post-peak load carrying capacity, which indicates that assuming some debond between FRP grid and surrounding HPFRC seems relevant for assuring higher accuracy on the modelling performance.

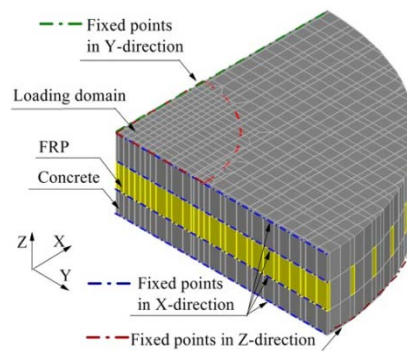


Fig. 9: Three-dimensional finite element model of a manhole cover

Tab. 6: Parameters of the concrete constitutive models adopted for the model. Type of shear retention law for FRP:  $P_1=2$

Property	HPFRC	Plain Concrete	FRP
Poisson's ratio ( $\nu$ )	0.2	0.15	0.15
Young's modulus ( $E$ )	32000 $N/mm^2$	27000 $N/mm^2$	14000 $N/mm^2$
Compressive strength ( $f_c$ )	60.0 $N/mm^2$	60 $N/mm^2$	30 $N/mm^2$
Trilinear tension-softening diagram	$f_{ct} = 2.8 N/mm^2$ $G_f^1 = 3 N/mm$ $\xi_1 = 0.005; \alpha_1 = 0.78$ $\xi_2 = 0.058; \alpha_2 = 0.89$ $\xi_3 = 0.36; \alpha_3 = 0.57$	$f_{ct} = 1.7 N/mm^2$ $G_f^1 = 0.07 N/mm$ $\xi_1 = 0.005; \alpha_1 = 0.3$ $\xi_2 = 0.3; \alpha_2 = 0.2$	$f_{ct} = 170 N/mm^2$ $G_f^1 = 1000 N/mm$ $\xi_1 = 0.005; \alpha_1 = 0.3$ $\xi_2 = 0.3; \alpha_2 = 0.2$
Crack shear stress-crack shear strain softening diagram	$\tau_{t,p}^{cr} = 1.5 N/mm^2; \beta =$ $G_{f,s} = 1 N/mm;$	-	-
Threshold angle	30°	30°	30°

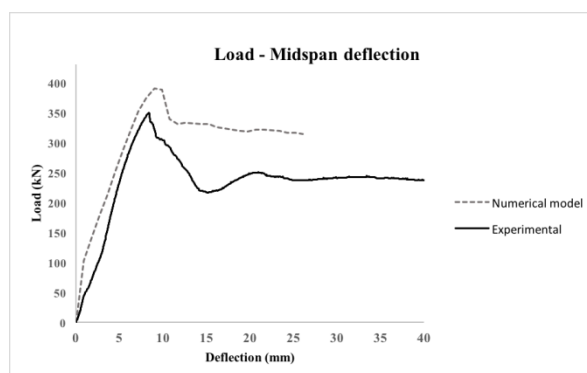


Fig. 10: Experimental and numerical results in terms of load versus deflection.

#### 4. Conclusions

Two types of concrete mixtures were evaluated along with a FRP grid reinforcement system in order to constitute an alternative solution for manhole covers currently made of steel or steel reinforced concrete. In this program, four specimens were submitted to a compressive point load to assess their maximum load carrying capacity and compare these values with the values defined by the EN-124, in order to establish an appropriate class of utilization for the production of precast manhole covers.

A high increase in the load carrying capacity has been observed in specimens of HPFRC and with higher thickness in the upper concrete layer (above the FRP reinforcement). The specimens of 100mm thickness of both mixtures: HPFRC-T100-C30 and DHCC-T100-C15, showed better elastic and post peak ductile behaviour and reached to maximum loads of 349.36 kN and 156.32 kN respectively, which corresponds to manhole covers of class C250 and class B125, according to the CEN. EN 124:1994.

A suitable interaction concrete-FRP reinforcement has been observed in the HPFRC specimens, along with a better filling of the concrete mix in the spaces between the grid.

Numerical simulation of the specimen with higher load carrying capacity (class C250) has been carried on. The model was capable to capture with relative accuracy the flexural response of this specimen. The minor deviation of results suggests that debonding between concrete and the FRP system should be considered.

#### Acknowledgements

*The authors would like to acknowledge the cooperation of the European Regional Development Fund (FEDER) through the Operational Program North for the funding of the research project No. 30367 UrbanCrete – Betão Reforçado com Fibras de Características Melhoradas de Durabilidade para Aplicação em Mobiliário Urbano.*

#### References

- [1] “The World of Street Crime Has an Increasingly Popular Target: Manhole Covers”. The New York Times Ed. May 4th (2012), page A22
- [2] “Stolen manhole covers put lives at risk”. The Niagara Falls review, April 25th (2012).

- [3] “China manhole thefts prove deadly”. BBC News, Asia-pacific Ed. Jan 29<sup>th</sup> (2004).
- [4] SOLTANZADEH F., BARROS J.A.O., SANTOS R.F.C., *Construction and Building Materials* 77 (2015) 94-109. doi:10.1016/j.conbuildmat.2014.12.003
- [5] Mastali M, Valente IB, Barros JAO. “New composite slab system for the structural rehabilitation of traditional buildings. 11th Int Symp on FRP for Reinforced Concrete Structures. Guimarães, Portugal (2013).
- [6] CEN. EN 124:1994. Gully tops and manhole tops for vehicular and pedestrian areas - Design requirements, type testing, marking, quality control (1994).
- [7] Sena-Cruz JM. Strengthening of concrete structures with near-surface mounted CFRP laminate strips [Ph.D. thesis]. Guimarães, Portugal: University of Minho; 2004.
- [8] Ventura-Gouveia A. Constitutive models for the material nonlinear analysis of concrete structures including time dependent effects [Ph.D. thesis]. Guimarães, Portugal: University of Minho; 2011.